4．バルビツレート

中脳網様体賦活系などに作用し，鎮静・催眠から全身麻酔まで，中枢抑制のすべての段階に使用しうる。しかし，用量依存性の進行性中枢神経機能抑制作用を示す性質から呼吸抑制の危険性が高いこと，翌日への効果の持ち越し，精神機能の抑制などが問題としてあげられ，検査にあたっての鎮静としては慎重を要する。代表的なものとして以下の薬剤がある。

1）**ペントバルビタール**（pentobarbital）

通常量：0.5～1.0 mg/kg（静注）

作用時間は1～3時間と短い。

2）**チアミラール**（thyamylal），**チオペンタール**（thiopental）

通常量：1～5 mg/kg（静注）

作用時間は5～15分である。喘息患者には禁忌である。

5．抗ヒスタミン薬

ヒドロキシジン（hydroxyzine，アタラックスP®）

通常量：0.5～1.0 mg/kg（経口）

0.25～1.0 mg/kg（静注）

作用時間は経口で4～8時間，静注で1～4時間である。アジュバンド効果を有し，他の鎮静薬の効果を増強する。

6．**ケタミン**（ketamine，ケタラール®）

通常量：0.1～0.5 mg/kg（静注）

作用時間は5～15分である。鎮痛作用をもち，疼痛を伴う処置（骨髄穿刺など）における鎮静に有効である。しかし，副作用として脳圧亢進，気道口腔内分泌物の増加があげられ，副作用の点より検査目的での鎮静には適さない。NMDA受容体の非競合的拮抗が主な作用機序である。

7．**プロポフォール**（propofol）

通常量：1～3 mg/kg（静注）

非バルビタール静脈麻酔薬で深鎮静にも使用しうるが，呼吸抑制に対する対応が必須である。作用時間は5～10分と超短時間作用性であり，中止後のもうろう状態が少ないのが利点である。

ま と め

診断のために必要な検査であっても，患者のリスクを無視してまでも鎮静を行うという考えには異論を唱えるべきと考える。小児患者にいかに安全な医療を提供するか，その一環としてどのような鎮静を考えればよいかを常に念頭においた対応が望まれる。

文 献

1) Kaplan RF, Yang CI：Sedation and analgesia in pediatric patients for procedures outside the operating room. Anesthesiol Clin North America 20：181-193, 2002
2) American Academy of Pediatrics Committee on Drugs：Guidelines for monitoring and management of pediatric patients during and after sedation for diagnostic and therapeutic procedures. Pediatrics 89：1110-1115, 1992
3) An updated report by the American society of anesthesiologists task force on sedation and analgesia by non-anesthesiologists：Practice guidelines for sedation and analgesia by non-anesthesiologists. Anesthesiology 96：1004-1017, 2002
4) Jastak JT, Pallasch T：Death after chloral hydrate sedation：report of case. J Am Dent Assoc 116：345-348, 1988

* * *

ELSEVIER

Brain & Development 26 (2004) 37–42

BRAIN & DEVELOPMENT
Official Journal of the Japanese Society of Child Neurology

www.elsevier.com/locate/braindev

Original article

Context-dependent reasoning in a cognitive bias task Part II. SPECT activation study

Hitoshi Shimoyama[a], Masao Aihara[a,*], Hidenao Fukuyama[b], Kazuo Hashikawa[b], Kakurou Aoyagi[a], Elkhonon Goldberg[c], Shinpei Nakazawa[a]

[a]*Department of Pediatrics, Faculty of Medicine, University of Yamanashi, 1110 Tamaho-cho, Nakakomagun, Yamanashi 409-3898, Japan*
[b]*Department of Functional Brain Imaging, Human Brain Research Center, Graduate School of Medicine, Kyoto University, Kyoto, Japan*
[c]*Department of Neurology, New York University School of Medicine, New York, NY, USA*

Received 29 January 2003; received in revised form 14 April 2003; accepted 14 April 2003

Abstract

A cognitive bias task (CBT) delineates two different cognitive selection mechanisms in the prefrontal cortex. To identify functional anatomy of context-dependent reasoning, we used technetium-^{99m}hexamethyl- propyleneamine oxime (^{99m}Tc HM-PAO) single photon emission computed tomography (SPECT) and statistical parametric mapping. Twelve right-handed men 20–24 years old were instructed to look at a target card and then select the choice card (among two) that they preferred (modified CBT; mCBT). They also selected a choice card 2 weeks later without prior presentation of a target card (control task). In both tasks, ^{99m}Tc HM-PAO was injected intravenously about 15 s after initiation of the mCBT or control task. Brain images were obtained using a gamma camera and reconstructed by a UNIX-based workstation. Statistical analysis compared all activated images to control images. Results associated with P values of less than 0.01 (Z score >2.36) were depicted on T_1-weighted magnetic resonance images. All subjects preferred choices more similar to the target. SPECT activation occurred bilaterally in the dorsolateral prefrontal cortices and middle temporal gyri during performance of the CBT. Additionally, the left inferior prefrontal cortex and left fusiform gyrus showed significant activation compared with the control task. A neural network linking the temporal and prefrontal cortices prominently seen in the left hemisphere participates in context-dependent reasoning. Knowledge of such neural systems is essential for understanding prefrontal lobe function and dysfunction.
© 2003 Elsevier B.V. All rights reserved.

Keywords: Cognitive bias task; Context-dependent reasoning; Activation study; Single-photon emission computed tomography (SPECT); Statistical parametric mapping (SPM); Frontal lobe; Prefrontal lobe

1. Introduction

The prefrontal cortex has two cognitive selection mechanisms. One processing mechanism carries out exploratory processing of novel cognitive situations (context-independent reasoning), while the other carries out processing based on pre-existing representations (context-dependent reasoning) [1–3]. Goldberg et al. [4] recently described context-dependent and context-independent selection as respectively associated with the left and right frontal lobe, in right-handed male adults. Patients with left frontal lobe lesions showed context-independent reasoning in a cognitive bias task (CBT), while those with a right frontal lesion showed context-dependent reasoning. The shift accompanying routinization in the intact brain offers a dynamic view of lateralization of the frontal lobe. Aihara et al. have revealed that among right-handed male subjects, young children showed context-independent responses in a modified CBT (mCBT), while adolescents and adults showed context-dependent responses [5]. Thus, the locus of cortical control shifts from the right to the left frontal lobe as cognitive contextual reasoning develops. Accordingly, the CBT would be a highly informative cognitive activation task for imaging to lateralize function in the frontal lobes, providing a dynamic view of hemispheric specialization in terms of both laterality and region. However, the CBT has not been used in functional neuroimaging studies.

Functional neuroimaging has revealed much concerning brain function in perception and cognition [6,7]. At the same

* Corresponding author. Tel.: +81-55-273-9606; fax: +81-55-273-6745.
E-mail address: maihara@res.yamanashi-med.ac.jp (M. Aihara).

0387-7604/03/$ - see front matter © 2003 Elsevier B.V. All rights reserved.
PII: S0387-7604(03)00092-5

time, the frontal lobe has been implicated increasingly in developmental disturbances such as autistic disorder and attention deficit/hyperactivity disorder (ADHD) [8–10]. In this study we sought to identify the functional anatomy of context-dependent reasoning, using technetium-^{99m} hexamethyl-propyleneamine oxime (^{99m}Tc HM-PAO) single-photon emission computed tomography (SPECT) and statistical parametric mapping (SPM99).

2. Methods

2.1. Subjects

Twelve volunteers (all male; ages, 20–24 years) participated in this study. All subjects were right-handed [11], and had no history of psychiatric or neurologic illness. Informed consent was obtained from all subjects after the details of the study had been explained. The design of this study was approved by the ethical committee of the University of Yamanashi.

2.2. Task design

Goldberg et al. [4] proposed the CBT as a way to discriminate between left and right frontal lobe function. We used mCBT designed for children. The mCBT cards showed four characteristics: shape (circle or square), number (one or two), color (red or blue), and shading (unshaded outline or filled). At first one target card was presented. Two choice cards then were presented below the target card after 2 s. The subjects were instructed to look at the target card and then select a choice card according to their own preference. The 30 trial sequences that followed were the same for all subjects. As a control task, the subjects selected one of the two choice cards at random without prior presentation of a target card.

The mCBT raw score for each choice could range from 0 to 4 points. For example, if shape, color, and number but not shading were matched between the target card and the choice card, the raw score was 3 points. The overall mCBT raw score was the sum of similarity indices across trials, ranging from 30 to 90 points. High or low raw scores implied consistently similar choices (target-driven selection bias), while a middle-range score (around 60) implied that the choices were unrelated to the target (indifferent selection bias).

2.3. Imaging procedures

All subjects underwent both mCBT and control SPECT studies separated by an interval of 2 weeks. In both studies, technetium-^{99m} HM-PAO (370–740 MBq) was injected intravenously about 15 s after initiation of the mCBT or control task.

Brain images were obtained using a whole-body annular crystal gamma camera (Toshiba GCA-9300A/DI; Tokyo, Japan) equipped with low-energy, high-resolution three-head collimators. SPECT studies were acquired for 10 min in a 128 × 128 matrix with four degrees per second of continuous angular increment. These image reconstructions were performed at a UNIX-based workstation (Toshiba GMS-5500A Workstation; Tokyo, Japan).

2.4. Statistical parametric mapping

Analysis of data was performed by a personal computer with a Windows 2000 Professional Operating System using Statistical Parametric Mapping 99 software (SPM99; Institute of Neurology, University College of London, UK) [12]. The SPECT data reconstructed with attenuation and scatter collection were reformatted into the Analyze header format (Mayo Foundation, Baltimore, MD). SPECT images of each subject were co-registered between the activated and resting condition images. The data were then normalized to a high-resolution T1 template (Montreal Neurological Institution or MNI template) in lieu of our ^{99m}HM-PAO SPECT template to remove variation caused by differences in size and shape of individual brains, and smoothed with 8 mm full width at half maximum (FWHM) prior to SPM statistical analysis in order to improve statistical power by removing noise of the data. Statistical analysis was performed to compare all activated scans with all control scans. The results of t statistics were transformed to Z scores. The results were rendered on the reference T_1-weighted magnetic resonance images when P values were less than 0.01 (Z score, >2.36) with multiple comparison correction. For presentation, activated sections were rendered as hot-color maps on a three-dimensional surface view of the brain and also depicted on transverse slices.

3. Results

3.1. Behavioral data

All subjects performed the tasks well. Scores for each subject in the mCBT task exceeded 80 points (range, 82–90), which indicated that subjects responded in a highly context dependent-manner. The score for each subject in the control task was approximately 60 (range, 56–63), which reflected a context-independent mode of response.

3.2. SPECT activation data

CBT induced increased activation in a network system including right and left dorsolateral prefrontal cortices, right and left middle temporal areas, and the left insula and post-temporal area (Fig. 1). Exact locations as determined with Talairach coordinates are shown in Table 1.

Compared with the control task, CBT bilaterally

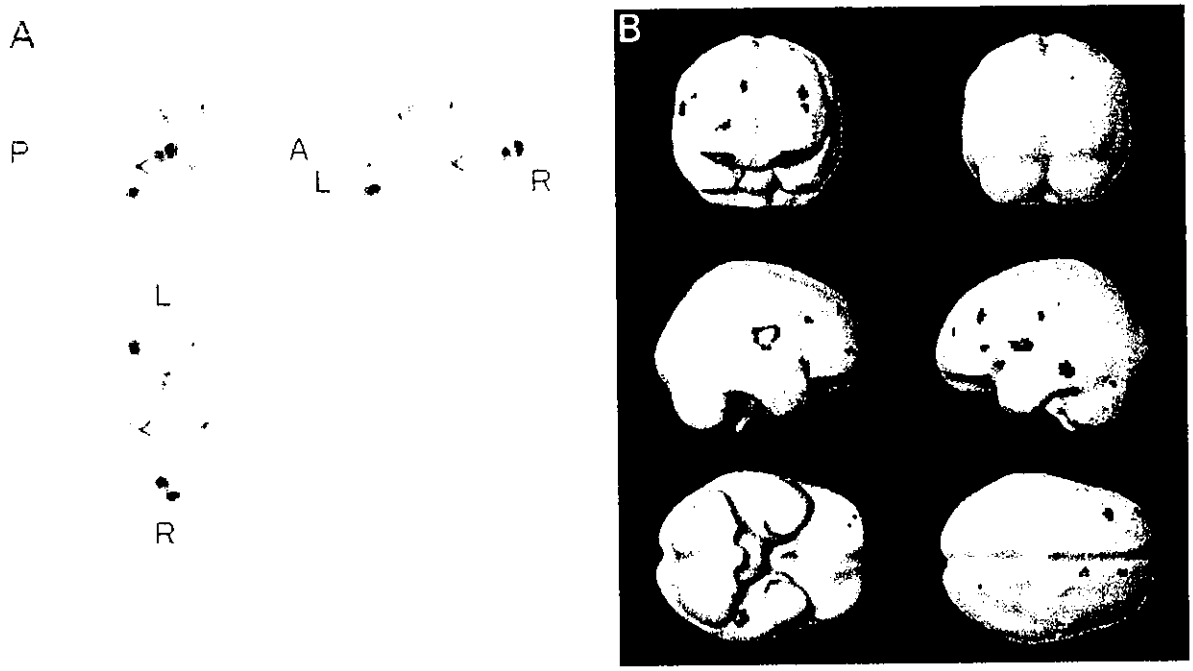

Fig. 1. Statistical parametric mapping (SPM). (A) Areas of significant activation ($P < 0.01$, corrected) are shown as a projection onto the glass brain. Coronal, viewed from behind; transverse, viewed from above; sagittal, viewed from right. (B) Surface SPM (Z) rendering images are superimposed upon three-dimensional magnetic resonance images. Activated regions are displayed in a 'hot' color.

activated the dorsolateral prefrontal cortices (BA 9/10/46) and the middle temporal gyri (BA 21/22); (Table 1; Fig. 2A,B). Activation also was significant in the left inferior prefrontal cortex (BA 45/47); (Table 1; Fig. 2B), the left premotor cortex (BA 6/24); (Table 1; Fig. 2C), and the left fusiform gyrus (BA 37); (Table 1; Fig. 2D).

4. Discussion

Traditional intelligence tests measure convergent thinking in the sense that a question usually has only one correct answer [13]. Tests of divergent thinking, in contrast, emphasize number and variety of answers to a single question. As CBT in our study requires divergent thinking, CBT was a multiple-choice response selection paradigm where preference rather than accuracy was examined. This mode of thinking has been reported to be particularly compromised by frontal lobe injury [13]. Performance of CBT by right-handed men with right prefrontal lesions showed an extreme response bias [4]. A group with left-sided lesions showed an opposite response bias. These findings suggest that left and right prefrontal systems exhibit different response selection biases: those guiding behavior according to internal context-based principles, and those using external environment-based principles [4]. In our mCBT study, all subjects preferred the choice most similar to the target. Therefore, we believe that our subjects selected one of the two choice cards based on internal context ordering hypothesized to involve the left prefrontal cortex in right-handed males.

Podell et al. [14] proposed that a CBT offers distinct advantages as a cognitive activation task for functional neuroimaging of the frontal lobes, since CBT discriminates well between the effects of left and right frontal lesions but still requires less time to administer, is easier to understand, and is better tolerated by subjects than the Wisconsin card sorting test (WCST), the current 'gold standard' for testing frontal lobe function. For functional neuroimaging, we chose a control task omitting presentation of a target card as an appropriate subtraction task for use with the CBT. This control task does not require the subject to make any 'most similar' or 'most different' choice. Operationally, the control task is identical to the CBT except for the presentation of the target card and subsequent divergent thinking, which are removed. With these task designs we could isolate response selection strategies and relate them to brain structures through SPECT activation imaging.

In this study the dorsolateral prefrontal cortices and middle temporal gyri were activated bilaterally as right-handed men performed the inherently ambiguous CBT. The left inferior prefrontal cortex and left fusiform gyrus also were significantly activated. Though clinical evidence has shown two functionally and neurally distinct cognitive selection biases [1,2], this study apparently is the first to show functional neuroimaging evidence of a neural system for context-dependent reasoning by healthy volunteers in a CBT.

According to CBT studies by Goldberg et al. [4,15],

Table 1
Areas showing activation

Location	Brodmann area	Talairach coordinates			Z-score
		x	y	z	
L. temporal lobe, middle temporal gyrus	21 22	−44	−35	−5	3.44
R. temporal lobe transverse temporal gyrus	41 42 21 22	51	−17	17	3.35
L. frontal lobe, precentral gyrus	6 24	−24	−12	41	2.97
L. frontal lobe, superior frontal gyrus	6	−46	−14	32	2.82
L. frontal lobe, superior frontal gyrus	10	−38	55	17	2.75
L. frontal lobe, middle frontal gyrus	10 46				
L. frontal lobe, inferior frontal gyrus	45 46 47	−44	29	6	2.7
L. frontal lobe, middle frontal gyrus	9	−36	34	28	2.69
L. frontal lobe, superior frontal gyrus	9				
R. frontal lobe, superior frontal gyrus	9	12	44	35	2.63
L. temporal lobe, fusiform gyrus	37	−51	−73	−17	2.58
R. frontal lobe, superior frontal gyrus	10	26	51	3	2.58
R. frontal lobe, middle frontal gyrus	10				
R. frontal lobe, middle frontal gyrus	46 9	53	23	26	2.47
R. frontal lobe, inferior frontal gyrus	9				
R. frontal lobe, middle frontal gyrus	10	34	56	1	2.35

lateralized prefrontal lesions in right-handed males differentially alter performance: right frontal lesions produce context-dependent responses, while left-sided lesions result in context-independent response. Whether there is a right-to-left shift of frontal advantage as the function of learning remains to be determined in this SPECT activation study. In our recent electrophysiologic study, however, the EEG spectral power increased in the gamma frequency bands (30–40 Hz) from the right to the left prefrontal regions as the CBT became familiar [16]. Recent investigations have reported that synchronization in the gamma band reflects a processing mode or working cortex [17,18]. In addition, this dual phenomenon was dramatically demonstrated by Gold et al. [19]. Using PET, they studied changes in blood flow patterns in the course of performing complex 'delayed alternating response' task. At the early learning stage the activation was greater in the right prefrontal regions than in the left. At the late stage the pattern was reversed: there was more activation in the left than right prefrontal regions [20]. Therefore, our results suggest that context-dependent reasoning in a CBT requires not only activation of both prefrontal lobes, but also dynamic changes of activation from the right to the left prefrontal lobes: the right prefrontal lobe (BA 9/10/46) is activated during the early portion of 30-CBT trials, followed in later trials by left prefrontal lobe (BA 9/10/46) activation associated with working memory. All subjects responded in an extremely context-dependent manner. These findings also support the hypothesis that the locus of cortical control shifts from right to left prefrontal over the course of cognitive skill development [15], as seen for cognitive contextual reasoning development [5]. Ongoing investigation of these issues in our laboratory includes analysis of transient shift-related signals in a CBT by using the temporal resolution of event-related functional magnetic resonance imaging method.

Our mCBT cards differed dichotomously in four respects: shape, color, number, and shading. Thus, subjects were required to discriminate 16 different visual objects as they preferred. In this respect, the CBT is a visual categorization task. In a previous investigation, Sigala and Logothetis examined neural mechanisms of categorization learning in macaque monkeys, finding that neural activity in

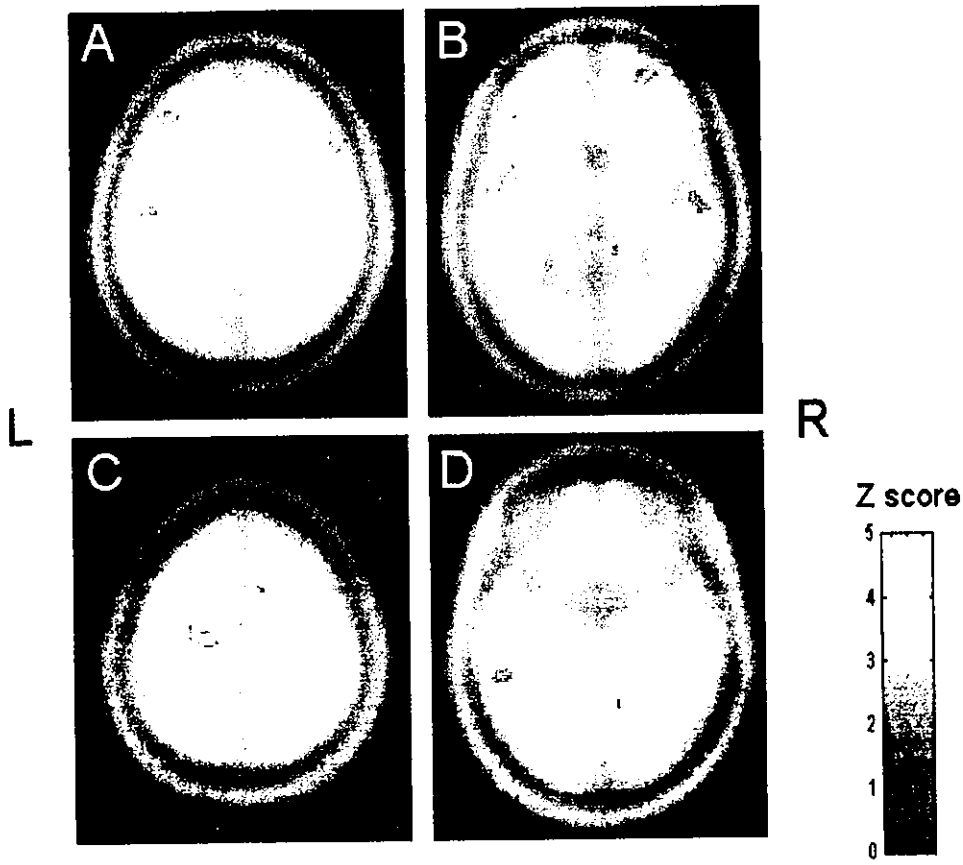

Fig. 2. Transverse statistical parametric mapping (Z) maps are superimposed upon magnetic resonance image. Coordinates are described with reference to the Talairach system. The local maximum within the activated volume is defined by the 'hot' color corresponding to (A) the left superior frontal gyrus ($x = -38$, $y = 55$, $z = 17$; $P < 0.01$, corrected; Z-score = 2.75); (A) the right superior frontal gyrus ($x = 26$, $y = 51$, $z = 3$; $P < 0.01$, corrected; Z-score = 2.58); (B) the left middle temporal gyrus ($x = -44$, $y = -35$, $z = -5$; $P < 0.01$, corrected; Z-score = 3.44); (B) the right transverse temporal gyrus ($x = 51$, $y = -17$, $z = 17$; $P < 0.01$, corrected; Z-score = 3.35); (C) the left middle frontal gyrus ($x = -24$, $y = -12$, $z = 41$; $P < 0.01$, corrected; Z-score = 2.97); and (D) the left fusiform gyrus ($x = -51$, $y = -73$, $z = -17$; $P < 0.01$, corrected; Z-score = 2.58).

the inferior temporal cortex was significantly enhanced during categorization in combined psychophysical and electrophysiologic experiments [21]. In humans, fine-grained categorization is selectively impaired after lesions that include the fusiform gyrus [22,23]. These findings indicate that activation of the temporal lobes, especially the fusiform gyrus, is critical for a visual categorization task such as CBT. Just after mCBT, on the other hand, all subjects had easy answering questions that probe the information of both target and choice cards presented lastly. In addition, it has been well known that the patients with damage to left fusiform gyrus are impaired at naming and retrieving information about visual objects [24,25]. These findings could provide an explanation why the left (not right) fusiform gyrus was activated by mCBT.

Prefrontal activation also has been correlated closely with a categorization task [26–28]. Hasegawa and Miyashita postulated that conceptual categorization is likely to depend on a neural network distributed between prefrontal and posterior association cortex, possibly including linguistic areas [22]. Activations in the left inferior prefrontal cortex (BA 45/47) and the left premotor cortex (BA 6/24) might be part of a language-related process in CBT. The present data indicate first that context-dependent reasoning in mCBT requires activation of a distributed network and second that the location of these sites are not symmetrically distributed, but rather prominently distributed in the left hemisphere, evidenced by the selective activation of the left fusiform, premotor and inferior frontal regions. Thus, context-dependent reasoning in mCBT would require activation of both retrieving visual information and internal speech [29,30]. Studies showing selective activation of left frontal cortex for naming and retrieving information about objects provide additional support for this view [29,31]. The likely mechanism can be inferred from our experiment that demonstrated reciprocal interactions between temporal and prefrontal cortices prominently seen in the left hemisphere along bottom-up and top-down connections in CBT including memory recall, retrieval [32–34], categorization [21], performance monitoring [35], decision making [36], and contextual updating [34].

5. Conclusion

Using ^{99m}HM-PAO SPECT and SPM99, we identified a neural network between temporal and prefrontal cortices prominently seen in the left hemisphere linked to context-dependent reasoning in mCBT. More detailed knowledge of such neural systems is essential for understanding frontal lobe function and dysfunction.

Acknowledgements

Our research was supported in part by The Japan Epilepsy Research Foundation (M.A.).

References

[1] Goldberg E, Costa LD. Hemispheric differences in the acquisition and use of descriptive systems. Brain Lang 1981;14:144–73.
[2] Lhermitte F. 'Utilization behavior' and its relation to lesions of the frontal lobes. Brain 1983;106:237–55.
[3] Milner B, Petrides M. Behavioural effects of frontal lobe lesions in man. Trends Neurosci 1984;7:403–7.
[4] Goldberg E, Podell K, Harner R, Riggio S, Lovell M. Cognitive bias, functional cortical geometry, and the frontal lobes: Laterality, sex, and handedness. J Cogn Neurosci 1994;6:276–96.
[5] Aihara M, Aoyagi K, Goldberg E, Nakazawa S. Age shifts frontal cortical control in a cognitive bias task from right to left: Part I. Neuropsychological study. Brain Dev 2003 doi: S0387-76 04(03)00064-0
[6] Caviness Jr VS, Lange NT, Makris N, Herbert MR, Kennedy DN. MRI-based brain volumetrics: emergence of a developmental brain science. Brain Dev 1999;21:289–95.
[7] Dong Y, Fukuyama H, Honda M, Okada T, Hanakawa T, Nakamura K, et al. Essential role of the right superior parietal cortex in Japanese kana mirror reading: An fMRI study. Brain 2000;123:790–9.
[8] Gorenstein EE, Mammato CA, Sandy JM. Performance of inattentive-overactive children on selected measures of prefrontal-type function. J Clin Psychol 1989;45:619–32.
[9] Swanson J, Castellanos FX, Murias M, LaHoste G, Kennedy J. Cognitive neuroscience of attention deficit hyperactivity disorder and hyperkinetic disorder. Curr Opin Neurobiol 1998;8:263–71.
[10] Happe F, Ehlers S, Fletcher P, Frith U, Johansson M, Gillberg C, et al. 'Theory of mind' in the brain. Evidence from a PET scan study of Asperger syndrome. Neuroreport 1996;8:197–201.
[11] Chapman LJ, Chapman JP. The measurement of handedness. Brain Cogn 1987;6:175–83.
[12] Nagayama Y, Fukuyama H, Yamauchi H, Matsuzaki S, Konishi J, Shibasaki H, et al. Cerebral activation during performance of a card sorting test. Brain 1996;119:1667–75.
[13] Milner B. Aspects of human frontal lobe function. In: Jasper HH, Riggio S, Goldman-Rakic PS, editors. Epilepsy and the functional anatomy of the frontal lobe. New York: Raven; 1995. p. 67–84.
[14] Podell K, Lovell M, Zimmerman M, Goldberg G. The cognitive bias task and lateralized frontal lobe functions in males. J Neuropsychiatry Clin Neurosci 1995;7:491–501.
[15] Goldberg E, Podell K. Lateralization in the frontal lobes. In: Jasper HH, Riggio S, Goldman-Rakic PS, editors. Epilepsy and the functional anatomy of the frontal lobe. New York: Raven; 1995. p. 85–96.
[16] Kamiya Y, Aihara M, Osada M, Ono C, Htakeyama K, et al. Electrophysiologic study of lateralization in the frontal lobes (in Japanese). Jpn J Cogn Neurosci 2002;3:188–91.
[17] Tallon-Baudry C, Bertrand O. Osillatory gamma activity in humans and its role in object representation. Trends Cogn Neurosci 1999;3: 151–62.
[18] Crone NE, Boatman D. Induced electrocorticographic gamma activity during auditory perception. Clin Neurophysiol 2001;112:565–82.
[19] Gold JM, Berman KF, Randolph C, Goldberg TE, Weinberger D. PET validation of a novel prefrontal task: delayed response alteration. Neuropsychology 1996;10:3–10.
[20] Goldberg E. The executive brain: frontal lobes and the civilized mind. New York: Oxford University Press; 2001.
[21] Sigala M, Logothetis NK. Visual categorization shapes feature selectivity in the primate temporal cortex. Nature 2002;415:318–20.
[22] Hasegawa I, Miyashita Y. Categorizing the world: expert neurons look into key features. Nat Neurosci 2002;5:90–1.
[23] Doran RJ, Fink GR, Rolls E, Booth M, Holmes A, Frackowiak RSJ, et al. How the brain learns to see objects and faces in an impoverished context. Nature 1997;389:596–9.
[24] Geschwind N, Fusillo M. Color-naming defects in association with alexia. Arch Neurol 1966;15:137–46.
[25] Damasio AR, Yamada T, Damasio H, Corbett J, McKee J. Central achromatopsia: behavioral, anatomic, and physiologic aspects. Neurology 1980;30:1064–71.
[26] Fuster JM. Executive frontal functions. Exp Brain Res 2000;133: 66–70.
[27] D'Esposito M, Ballard D, Zarahn E, Aguirre GK. The role of prefrontal cortex in sensory memory and motor preparation: An event-related fMRI study. Neuroimage 2000;11:400–8.
[28] Freedman DJ, Riesenhuber M, Poggio T, Miller EK. Categorical representation of visual stimuli in the primate prefrontal cortex. Science 2001;291:312–6.
[29] Grabowski TJ, Damasio H, Damasio AR. Premotor and prefrontal correlates of category-related lexical retrieval. Neuroimage 1998;7: 232–43.
[30] Gerlach C. Categorization and category effects in normal object recognition: a PET study. Neuropsychologia 2000;38:1693–703.
[31] Martin A, Wiggs CL, Ungerleider LG, Haxby JV. Neural correlates of category-specific knowledge. Nature 1996;379:649–52.
[32] Chao LL, Haxby JV, Martin A. Attribute-based neural substrates in temporal cortex for perceiving and knowing about objects. Nat Neurosci 1999;2:913–9.
[33] Buckner RL, Kelley WM, Petersen SE. Frontal cortex contributes to human memory formation. Nat Neurosci 1999;2:311–4.
[34] Shimamura AP. Memory retrieval and executive control process. In: Stuss DT, Robert TK, editors. Principles of frontal lobe function. London: Oxford University Press; 2002. p. 210–20.
[35] Gehring WJ, Knight RT. Prefrontal–cingulate interactions in action monitoring. Nat Neurosci 2000;3:516–20.
[36] Fuster JM. Overview of prefrontal functions: the temporal organization of behavior. The prefrontal cortex—anatomy, physiology and neuropsychology of the frontal lobe. 3rd ed. Philadelphia: Lippincott-Raven; 1997:209-252

ELSEVIER

Brain & Development 27 (2005) 148–151

BRAIN & DEVELOPMENT
Official Journal of the Japanese Society of Child Neurology

www.elsevier.com/locate/braindev

Original article

Sequential 3-D MRI frontal volume changes in subacute sclerosing panencephalitis

Hideaki Kanemura[a], Masao Aihara[a,*], Toshiyuki Okubo[b], Shinpei Nakazawa[a]

[a]*Department of Pediatrics, Faculty of Medicine, University of Yamanashi, 1110 Tamaho, Yamanashi 409-3898, Japan*
[b]*Department of Radiology, Faculty of Medicine, University of Yamanashi, 1110 Tamaho, Yamanashi 409-3898, Japan*

Received 26 November 2003; received in revised form 29 March 2004; accepted 9 May 2004

Abstract

In patients with subacute sclerosing panencephalitis, clinical stages defined according to Jabbour correlate strongly with frontal lobe dysfunctions. Nonquantitative radiologic investigations in these patients have confirmed cerebral atrophy without identifying predominantly affected regions. We addressed this issue over an 8-year-old boy's course using volumetry based on three-dimensional T1-weighted gradient echo magnetic resonance imaging. Seven normal 6–12-year-old subjects served as controls. Whole-brain volume declined as Jabbour stage advanced from I to III. Frontal lobe volume and frontal-to-whole-brain volume ratios fell significantly as clinical stage progressed. Thus, cerebral atrophy in this SSPE patient was predominantly frontal, and paralleled clinical progression.
© 2004 Elsevier B.V. All rights reserved.

Keywords: Subacute sclerosing panencephalitis (SSPE); Three-dimensional magnetic resonance imaging; Brain volumetry; Frontal lobe atrophy; Jabbour clinical stage

1. Introduction

Subacute sclerosing panencephalitis (SSPE), a rare, progressive, and frequently fatal infectious nervous system disease that affects children and young adults, is caused by an aberrant response to measles infection [1]. SSPE commonly is characterized by insidious onset of behavioral changes, emotional instability, and mental deterioration, followed by ataxia, myoclonic jerks, and focal neurologic signs [2]. A multidisciplinary study by Jabbour and coworkers [3] suggested a four-stage clinical classification that is used to evaluate disease progression. Clinical signs of SSPE such as emotional instability, behavioral changes, motor disturbances and myoclonic jerks correlate strongly with frontal lobe dysfunction.

Radiologic investigations using computed tomography (CT) and magnetic resonance imaging (MRI) in patients with SSPE confirmed cerebral atrophy [4,5], which is diffuse in the final stages of the disease [6]. However, the regions most severely involved were not identified in these qualitative studies.

We encountered a patient with SSPE who showed disturbance of motor function, lack of spontaneity, and emotional instability in his course. Marked improvement concerning emotional state and spontaneity occurred with long-term combined therapy with oral isoprinosine and intrathecal α-interferon. We serially measured total and frontal cerebral volumes by three-dimensional (3-D) MRI-based volumetry, correlating cerebral atrophy with clinical and laboratory data over time.

2. Case report

An 8-year-old boy was admitted to our hospital in November 1999 for evaluation of gait disturbance, dysarthria, and myoclonic jerks of the right upper limb. The second child of nonconsanguinous parents, he was born after an uneventful pregnancy and delivery and had normal motor and mental development up to the age of 8 years. Whether he had been infected with measles was unknown, but he had not received measles vaccine.

He showed lack of spontaneity and emotional instability. On neurologic examination he had myoclonic jerks of the right upper limb. Cranial nerve function was unremarkable.

* Corresponding author. Tel.: +81-55-273-9606; fax: +81-55-273-6745.
E-mail address: maihara@res.yamanashi-med.ac.jp (M. Aihara).

0387-7604/$ - see front matter © 2004 Elsevier B.V. All rights reserved.
doi:10.1016/j.braindev.2004.05.001

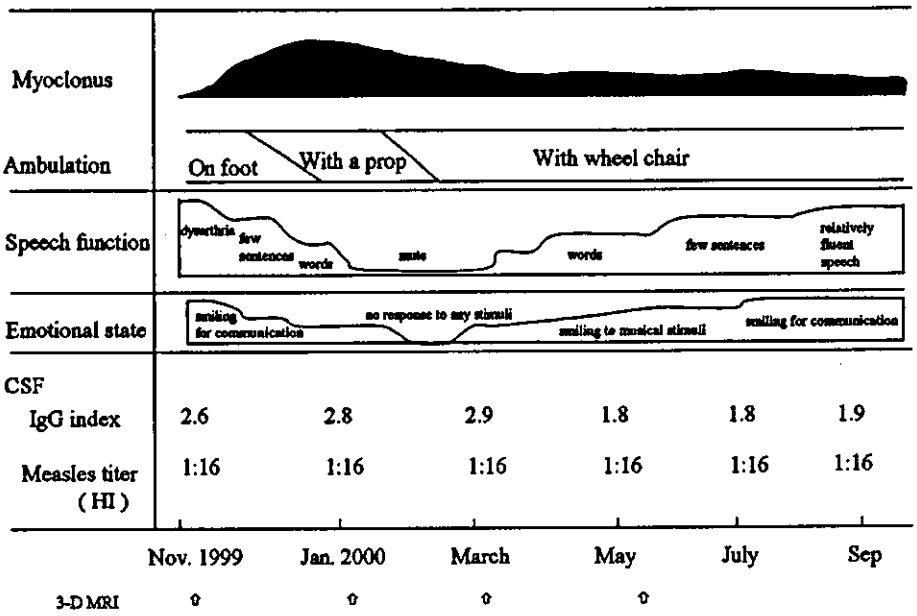

Fig. 1. Clinical course of a patient with SSPE. Symptoms rapidly progressed from Jabbour stage I to III, but improved to stage II by 6 months after initiating combination therapy. Measles titers in serum and cerebrospinal fluid showed no significant change throughout the course, but the IgG index changed in parallel with the clinical state. SSPE, subacute sclerosing panencephalitis; HI, hemagglutination inhibition.

Cogwheel rigidity was noted in the right limbs, where deep tendon reflexes were brisk. Results of routine hematologic and blood chemistry tests and urinalysis were normal. High measles antibody titers were found in serum (1:256) and cerebrospinal fluid (1:16). IgG was significantly elevated in the cerebrospinal fluid, as was the IgG index. Oligoclonal IgG bands were present in the cerebrospinal fluid. An electroencephalogram revealed periodic high-amplitude sharp- and slow-wave complexes. High-signal lesions were seen in the right parietal and occipital lobes on T2-weighted images. The patient was diagnosed with SSPE, and treatment was initiated immediately with combined oral isoprinosine and intrathecal α-interferon.

The patient's clinical course is shown in Fig. 1. He showed rapid progression from Jabbour stage I to III, followed by slow improvement from stage III to II. Initially ambulating unaided, he was wheelchair-bound or bedridden 2 months after onset of symptoms. He had not regained speech or responsiveness to stimuli at 3 months after initiation of therapy, and the Jabbour stage remained III. He regained responsiveness to stimuli and some speech 6 months after beginning combination therapy. Myoclonic jerks decreased in frequency, and emotional state was stable; improvement represented clinical stage II. Ambulation did not improve despite medical therapy and rehabilitation. Measles titers in cerebrospinal fluid showed no change throughout the course. On the other hand, the IgG index had changed from 2.6 at onset to 2.9 4 months later in association with clinical disease progression, but was 1.8 in association with clinical improvement at 6 months after onset. Routine MRI showed mild progression of brain atrophy and high signal intensity in subcortical white matter.

3. Serial 3-D MRI volumetry

Volumetric 3-D MRI evaluation was performed in the patient four times, at onset of symptoms and 2, 4, and 6 months after onset (Fig. 1).

A control group consisted of seven age-matched children, including five boys and two girls who ranged in age from 7 to 12 years (mean 9). Clinical indications for MRI included suspected speech delay, brain trauma, brain tumor, short stature, and migraine. No neurologic, cognitive, or emotional disorder was present in controls during 2–4 years of subsequent follow-up. No control subject had abnormal findings by routine MRI.

MRI was performed using a 1.5-Tesla system (GE, location). The 3-D MRI data were acquired by fast spoiled gradient recalled echo in a steady state with 3-D Fourier transformation. Images of the entire brain surface in 3-D were obtained from the 124 sections using an Advantage Windows RP 3-D analyzer (General Electric, Wisconsin, MW). Then frontal lobe was determined and confirmed using the same method as our previous report [7]. Finally we measured whole-brain and frontal lobe volumes using the volume measurement function of the analyzer workstation, based on the 3-D images.

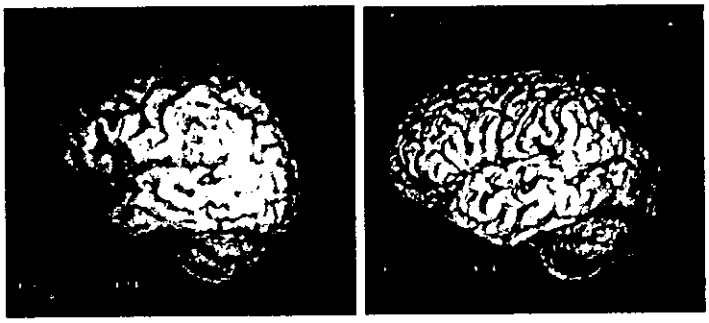

Fig. 2. Three-dimensional surface views of the left hemisphere 4 months after onset in a patient with SSPE (A) and in an age-matched normal control (B). SSPE, subacute sclerosing panencephalitis.

Fig. 2A depicts 3-D surface views of the patient's left hemisphere in comparison to those of a normal subject (Fig. 2B). The patient's frontal lobe was clearly atrophic to simple inspection. Serial MRI findings revealed increased signal on T2-weighted images in subcortical white matter, enlargement of lateral ventricles, and slowly progressive cerebral atrophy.

Measured volumes for whole brain and frontal lobe, and ratios of frontal lobe to whole-brain volume are shown in Fig. 3. Whole-brain volumes declined with progression of Jabbour stages from I to III remaining essentially unchanged thereafter during clinical improvement from stage III to II (Fig. 3A). Frontal lobe volume declined significantly with progression of clinical stage, then remaining constant (Fig. 3B). The frontal lobe to whole-brain volume ratio fell significantly with progression of clinical stage, and restored slightly during clinical improvement (Fig. 3C).

4. Discussion

Quantitation of volume is useful in characterizing normal brain growth as well as disturbances of growth caused by various diseases. Volumetric analysis of the brain may predict functions associated with the region measured. Using volumetry based on 3-D MRI, we investigated frontal and prefrontal normal growth during childhood and adolescence [7]. Reliability of MRI-based volumetric analysis reflects both image quality and the power of the analysis [8], as confirmed by comparison of direct and MRI volumetric measurements in cadaver brains. Furthermore, intra- and inter-rater variations were comparable to those in other studies [9].

Neuroimaging in the patients with SSPE is not absolutely required for diagnosis, but it offers important clues for clinical assessment. Reported distributions of MRI

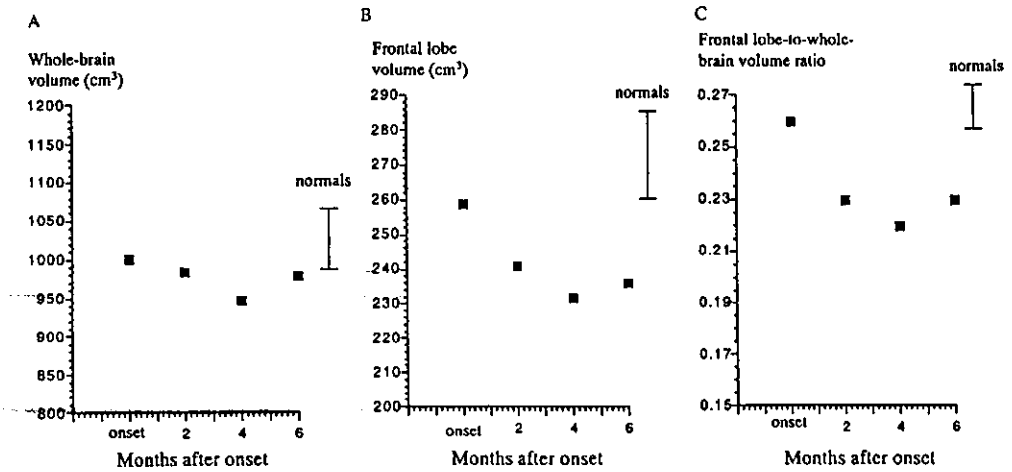

Fig. 3. Serial changes of whole brain volume (A), frontal lobe volume (B), and the frontal lobe to whole-brain volume ratio (C). Whole-brain volumes declined with progression of clinical stage according to Jabbour. Frontal lobe volume and the frontal lobe-to-whole-brain volume ratio also declined significantly with progression of clinical stage. Bars indicate the range for age-matched control patients who proved to have no neurologic disease.

abnormalities have varied between series [6,10,11]. Kulczycki et al. [12] found the inflammatory process to begin in occipital white matter and proceed toward the frontal region. As the disease progresses, lesions showing demyelination, necrosis, gliosis, and cerebral atrophy become increasingly prominent [10], as is best appreciated in T2-weighted images. However, correlations between clinical state and MRI findings have not been clear in previous reports [4,6,10]. Previous MRI studies performed at different stages of the disease [1,4,10,13,14] have suggested that SSPE can involve cortical gray matter, white matter, and basal ganglia, leading to atrophy. In previous reports mild atrophy was seen as early as 6 months, with subsequent progression [1]. In other reports, cerebral atrophy was observed in patients with a rapid disease course or an advanced disease stage [14]. Atrophy appears to result from postinflammatory tissue damage, and may occur earlier in patients with a relatively rapid course. Thus, the pattern of cerebral atrophy in a patient with SSPE can vary with clinical stage and duration of symptoms.

Symptoms of SSPE characteristically include an insidious onset of behavioral changes and emotional instability. Patients with frontal lesions also demonstrate a range of social impairments related to changes in personality and irresponsibility. Previous investigations have underscored the importance of the frontal cortex, especially the orbitofrontal cortex, in social interactions and emotional responses. On the basis of PET studies in SSPE, Huber et al. [15,16] hypothesized that inflammation associated with excessive metabolism in the basal ganglia interferes with connections between frontal, temporal, and parietal areas, resulting in Jabbour stage II symptoms. On the other hand, PET findings included decreased cerebral blood flow and oxygen metabolism in the frontal lobes [17], suggesting that frontal lobe function had a particularly strong correlation with clinical stage in SSPE.

To the best of our knowledge, no attempt has been made to measure individual cerebral lobes in patients with SSPE. Our study therefore may be the first to quantitate atrophy of the whole brain and frontal lobes in a patient with SSPE. Frontal lobe volumes, especially when considered as a ratio to whole-brain volume, decreased in association with advances of clinical stage and increases of the IgG index, and restored slightly with clinical improvements. Thus, cerebral atrophy in SSPE, particularly frontal lobe atrophy, might correlate with clinical and laboratory progression and improvement.

Clinical stage did not significantly reflect MRI findings when a heterogeneous group of SSPE patients was considered, although imaging findings correlated with clinical stage during the first year after onset [5]. Furthermore, serial MRI and clinical examinations carried out by Akdal et al. [18] exhibited little correlation between MRI findings and clinical stage. However, our patient showed a close relationship over time between frontal lobe atrophy and both the clinical state and the IgG index. Our investigation is the first to use quantitative and regional analysis based on 3-D MRI. In the future, investigations of the frontal lobe by serial 3-D MRI may have important role in clinical evaluation in SSPE.

In conclusion, our findings suggested that cerebral atrophy in a patient with SSPE occurred mainly in the frontal lobes and this technology may be a useful tool for understanding clinical dysfunctions of SSPE.

References

[1] Zeman W. Subacute sclerosing panencephalitis and paramyxovirus infections. In: Vinken PJ, Bryun GW, editors. Handbook of clinical neurology. Amsterdam: Elsevier; 1978. p. 343–68.

[2] Dyken PR. Subacute sclerosing panencephalitis. Neurol Clin 1985;3: 179–96.

[3] Ohya T, Martinez AJ, Jabbour JT, Lemmi H, Duenas DA. Subacute sclerosing panencephalitis. Correlation of clinical, neurophysiologic and neuropathologic findings. Neurology 1974;24:211–7.

[4] Brismar J, Gascon GG, Steyern KV, Bohlega S. Subacute sclerosing panencephalitis: evaluation with CT and MR. Am J Neuroradiol 1996; 17:761–72.

[5] Tuncay R, Akman-Demir G, Gokyigit A, Eraksoy M, Barlas M, Tolun R, et al. MRI in subacute sclerosing panencephalitis. Neuroradiology 1996;38:636–40.

[6] Anlar B, Saatci I, Kose G, Yalaz K. MRI findings in subacute sclerosing panencephalitis. Neurology 1996;47:1278–83.

[7] Kanemura H, Aihara M, Aoki S, Araki T, Nakazawa S. Development of the prefrontal lobe in infants and children: a three-dimensional magnetic resonance volumetric study. Brain Dev 2003;25:195–9.

[8] Caviness Jr. VS, Lange NT, Makris N, Herbert MR, Kennedy DN. MRI-based brain volumetrics: emergence of a developmental brain science. Brain Dev 1999;21:289–95.

[9] Aylward EH, Augustine A, Li Q, Barta PE, Pearlson GD. Measurement of frontal lobe volume on magnetic resonance imaging scans. Psychiatry Res 1997;75:23–30.

[10] Geller TJ, Vern BA, Sarwar M. Focal MRI findings in early SSPE. Pediatr Neurol 1987;3:310–2.

[11] Winer JB, Pires M, Kermode A, Ginsberg L, Rossor M. Resolving MRI abnormalities with progression of subacute sclerosing panencephalitis. Neuroradiology 1991;33:178–80.

[12] Kulczycki J, Kryst-Widzgowska T, Sobczyck W, Milewska D, Bochynska A. NMR and CT images in subacute sclerosing panencephalitis. Neurol Neurochir Pol 1994;28(suppl 1):79–90.

[13] Tsuchiya K, Yamauchi T, Fururi S, Suda Y, Takenaka E. MR imaging vs. CT in subacute sclerosing panencephalitis. Am J Neuroradiol 1988;9:943–6.

[14] Bohlega S, Al-Kawi MZ. Subacute sclerosing panencephalitis: imaging and clinical correlation. J Neuroimaging 1994;4:71–6.

[15] Huber M, Herholz K, Pawlik G, Szelies B, Jurgens R, Heiss W-D. Cerebral glucose metabolism in the course of subacute sclerosing panencephalitis. Arch Neurol 1989;46:97–100.

[16] Huber M, Pawlik G, Bamborschke S, Fink GR, Karbe H, Schlenker M, et al. Changing pattern of glucose metabolism during the course of subacute sclerosing panencephalitis as measured with ^{18}FDG-positron-emission tomography. J Neurol 1992;239:157–61.

[17] Yoshikawa H, Fueki N, Yoneyama H, Ogawa M, Sakuragawa N. Positron emission tomography demonstrated localized luxury perfusion in subacute sclerosing panencephalitis. J Child Neurol 1990;5: 311–5.

[18] Akdal G, Baklan B, Cakmakci H, Kovanlikaya A. MRI follow-up of basal ganglia involvement in subacute sclerosing panencephalitis. Pediatr Neurol 2001;24:393–5.

Case Report

Pediatric Neurosurgery

Pediatr Neurosurg 2004;40:230–233
DOI: 10.1159/000082297

Received: February 24, 2004
Accepted after revision: May 28, 2004

Intracranial Ectopic Recurrence of Craniopharyngioma after Ommaya Reservoir Implantation

Keisuke Ishii[a] Kenji Sugita[a] Hidenori Kobayashi[a] Tohru Kamida[a]
Minoru Fujiki[a] Tatsuro Izumi[b] Teruaki Mori[c]

Departments of [a]Neurosurgery and [b]Pediatrics, Oita University Faculty of Medicine, and
[c]Department of Neurosurgery, National Nishibeppu Hospital, Oita, Japan

Key Words
Craniopharyngioma · Total removal · Ectopic recurrence · Childhood · Ommaya reservoir

Abstract
We present a very rare case of a craniopharyngioma showing intracranial ectopic recurrence after the total removal of recurrent craniopharyngioma arising at the primary site accompanied by Ommaya reservoir implantation. A 2-year-old boy underwent a bifrontal craniotomy and total removal of the adamantinomatous craniopharyngioma via the interhemispheric translamina terminalis approach. Four months later, he underwent total removal of recurrent craniopharyngioma and implantation of an Ommaya reservoir via the same approach. Ten months later, total removal of the ectopic recurrent craniopharyngioma following the placement of the Ommaya reservoir cannula, which was placed within the surgical route, was performed via the same craniotomy.
Copyright © 2004 S. Karger AG, Basel

Introduction

Craniopharyngioma is a benign neoplasm that accounts for approximately 2–3% of all intracranial tumors and arises from the squamous epithelial nests of Rathke's pouch [1–3]. Complete tumor excision is difficult due to the peripheral structure. The recurrence of craniopharyngioma is not rare and often occurs at the primary site or in an adjacent area. However, the ectopic recurrence of craniopharyngioma is very rare, and to date, only 12 cases have been reported [4–15]. The authors present a case of craniopharyngioma showing intracranial ectopic recurrence after the total removal of recurrent craniopharyngioma arising at the primary site.

Case Report

A 2-year-old boy presented at the Pediatrics Department of his local hospital on April 5, 2000, with headache, nausea and lethargy persisting since the middle of March 2000. Computed tomography (CT) demonstrated a suprasellar mass extending to the third ventricle and acute hydrocephalus. The patient was referred to our hospital and was admitted the same day. No remarkable abnormal neurological findings were detected. On magnetic resonance imaging (MRI), the mass measured 2.0 × 2.0 × 4.0 cm, with both solid and cystic components (fig. 1). The solid component was heterogeneously enhanced and included calcification. The cyst wall was well enhanced.

KARGER
Fax + 41 61 306 12 34
E-Mail karger@karger.ch
www.karger.com

© 2004 S. Karger AG, Basel
1016–2291/04/0405–0230$21.00/0

Accessible online at:
www.karger.com/pne

Keisuke Ishii, MD, PhD
Department of Neurosurgery, Oita University Faculty of Medicine
1-1 Idaigaoka, Hasama-machi
Oita 879-5593 (Japan)
Tel. +81 97 586 5862, Fax +81 97 586 5869, E-Mail keisuke@med.oita-u.ac.jp

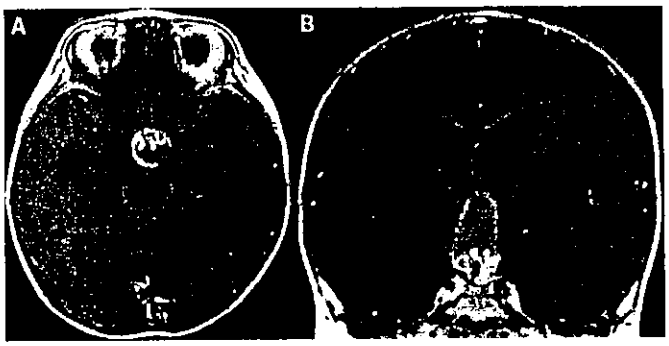

Fig. 1. Axial T_1-weighted gadolinium-enhanced (**A**) and coronal (**B**) MR images demonstrated a well-enhanced suprasellar mass extending to the third ventricle, and acute hydrocephalus. The mass measured 2.0 × 2.0 × 4.0 cm, with both solid and cystic components. The solid component was heterogeneously enhanced and included calcification. The cyst wall was well enhanced.

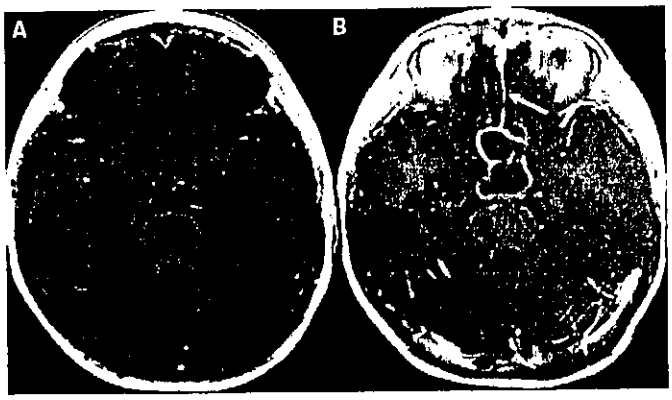

Fig. 3. Axial T_1-weighted gadolinium-enhanced MR images (**A**), 20 days after the initial surgery, revealed no residual tumor. Axial T_1-weighted gadolinium-enhanced MR images (**B**), 4 months after the initial surgery, revealed a recurrent tumor at the primary site and a trail of enhancement along the initial surgical tract (white arrow). This multilocular cystic mass measured 3.0 × 3.0 × 3.0 cm.

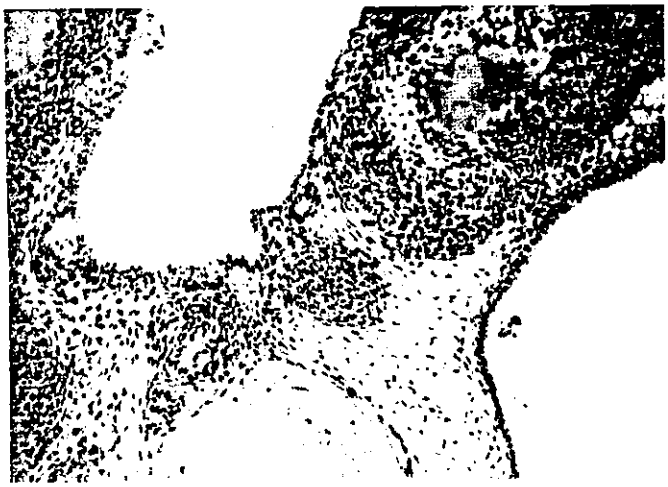

Fig. 2. Photomicrograph indicating a typical craniopharyngioma of the adamantinomatous type. Stratified squamous epithelium surrounding a loose 'reticulate' hypocellular region with multiple cysts and calcifications can be seen. HE. ×200.

Acute hydrocephalus was demonstrated, causing a mass on the third ventricle. We diagnosed craniopharyngioma and performed a bifrontal craniotomy with total removal of the tumor via the interhemispheric translamina terminalis approach on April 11. Histopathological examination confirmed the diagnosis of an adamantinomatous craniopharyngioma (fig. 2). MRI, 20 days after the first operation, revealed no residual tumor (fig. 3A). Postoperatively, the patient developed panhypopituitarism and diabetes insipidus. Thyroid hormone, an adrenal cortical hormone and an antidiuretic hormone were administered. No postoperative radiotherapy was administered. The patient was discharged without neurological deficits. Four months later, on August 28, the patient's mother noticed signs of visual impairment in her child. There had been no previous signs of visual impairment and he had not complained of this symptom until that time. He was extremely nearsighted, able to see only about 30 cm. MRI demonstrated recurrent suprasellar craniopharyngioma, a multilocular cystic mass measuring 3.0 × 3.0 × 3.0 cm (fig. 3B). The patient underwent total removal of the recurrent craniopharyngioma via the same approach. At this time, an Ommaya reservoir was implanted and the tip of the cannula was inserted into the extraction cavity for the management of future recurrence, for aspiration of the cystic component and reduction of the tumor mass. The histopathological examination was similar to that previously performed. Postoperatively, his visual impairment improved by degrees. However, CT on the sixth postoperative day demonstrated minute calcifications around the Ommaya reservoir cannula that had not been seen the day after surgery (fig. 4A, B). MRI after about 2 months demonstrated a cystic mass surrounding the Ommaya reservoir cannula in the center of the frontal base in the subdural space under the craniotomy bone flap (fig. 4C). After 6 months, CT revealed an enlarged well-enhanced cystic mass involving minute calcifications around the cannula (fig. 4D). On June 26, 2001, 10 months after the previous operation, total removal of the tumor was performed via the same craniotomy since this cystic lesion had grown gradually (fig. 5). The Ommaya reservoir cannula was removed from the recurrent tumor during the surgical procedure. There was no adherent tumor tissue, including calcification, and the histopathological features of the tumor were identical to those of the adamantinomatous craniopharyngioma that had been removed previously. There was no evidence of histological malignancy such as nuclear atypia, high mitotic activity or necrosis. The postoperative clinical course was good with no neurological deficits. Routine follow-up MRI 2 years and 7 months after the third operation revealed no evidence of recurrent tumor.

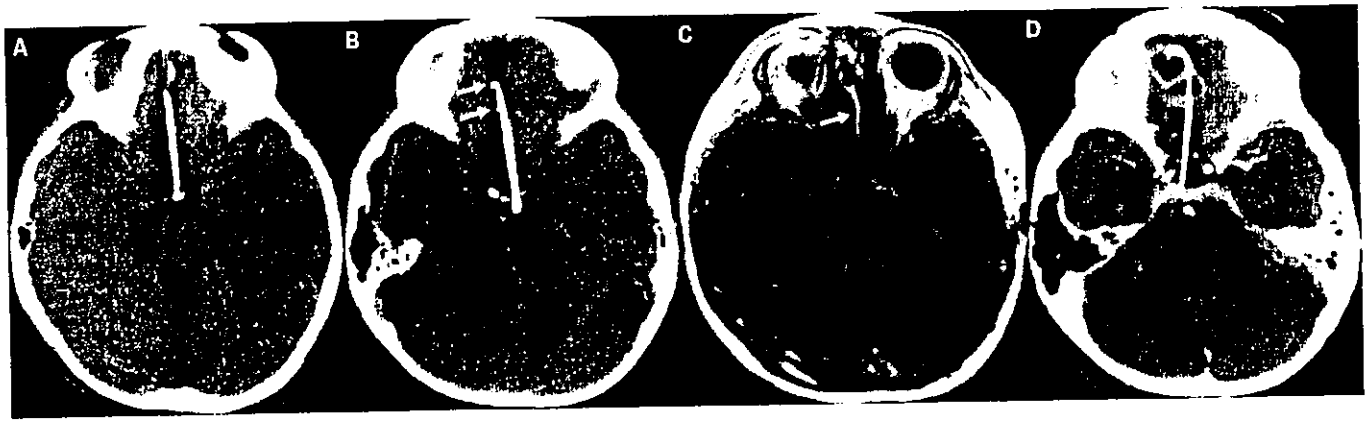

Fig. 4. Plain CT, the day after the previous (second) surgery (**A**), showed total removal of the tumor and no minute calcification around the Ommaya reservoir cannula. However, plain CT, 6 days after the previous (second) surgery (**B**), demonstrated minute calcification around the Ommaya reservoir cannula (white arrows). Axial T_1-weighted gadolinium-enhanced MR images, 2 months after the previous (second) surgery (**C**), demonstrated a cystic mass surrounding the Ommaya reservoir cannula in the center of the frontal base in the subdural space under the craniotomy bone flap. Enhancement along the Ommaya reservoir cannula was noted (white arrow). Enhanced CT, 6 months after the previous (second) surgery (**D**), demonstrated a multilocular cystic mass involving minute calcification surrounding the Ommaya reservoir cannula in the center of the frontal base.

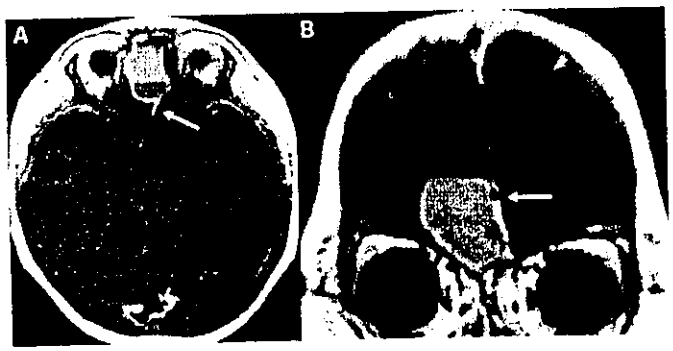

Fig. 5. Axial T_1-weighted gadolinium-enhanced (**A**) and coronal (**B**) MR images, 10 months after the previous (second) surgery, demonstrated a well-enhanced cystic mass. The enhanced lesion followed the Ommaya reservoir cannula. **A** Enhancement along the Ommaya reservoir cannula was noted (white arrow). **B** The wall of the cystic mass involving the cannula (white arrow).

Discussion

The ectopic recurrence of craniopharyngioma is a very rare postoperative complication and, to our knowledge, only 12 such cases have been reported [4–15]. Eight reports in the literature have described ectopic recurrence after the dissemination of residual tumor cells along the tract of the previous surgical route [4, 5, 7, 10–12, 14, 15]. Among these cases was 1 patient with an epidural mass [12] and 2 with masses in the sylvian cistern [10, 14]. In 4 other reports, ectopic recurrence was considered remote metastasis of the primary tumor by cerebrospinal fluid (CSF) dissemination because the site of the recurrent tumor was anatomically separate from both the primary site and the previous surgical route [6, 8, 9, 13]. One of these cases involved the spinal canal [9]. Nomura et al. [13] reported a case that clearly demonstrates CSF dissemination based on positive CSF cytology.

In our case, the ectopic recurrence was considered the dissemination of residual tumor cells along the tract of the previous surgical route, because the recurrent tumor was located along the line of the previous surgical approach. However, it presented unique aspects differing from the 12 previously reported cases. First, this patient was very young: in previous reports, the patients' age at presentation ranged from 10 [4] to 73 years [6], while age was not reported in 1 patient [15]. Second, the time to seeding was very short, only 2 months. In the 12 reported cases, remote recurrence was detected from 20 months [13] to 21 years [12] after the previous surgical intervention. In 1 of these cases, malignant transformation was detected [13]. Third, the tumor recurred along the Ommaya reservoir cannula, surrounding it and grew gradually. Bleyer et al. [16] presented a patient treated for meningeal Burkitt's lymphoma, and the cause of death was a large mass of tumor cells growing around the cannula. These authors considered that Burkitt's cells disseminated along the cannula track deeply into the brain parenchyma. In our case, unfortunately, the Ommaya reservoir cannula was acci-

dentally removed from the recurrent tumor during the craniotomy, but there was no adherent tumor tissue, including calcification. The cannula might have detached from the tumor capsule containing minute calcifications even though they were adjacent to each other in the preoperative radiological findings.

When did the ectopic recurrence begin, before or after the second operation in which the Ommaya reservoir cannula was inserted? Our hypothesis is that ectopic recurrence initiated before the second operation and became more obvious. A trail of enhancement along the initial surgical tract in MR images, 4 months after the initial surgery, could be considered the response to tumor recurrence, and supports our hypothesis. The intraoperative findings at the second surgery could not support ectopic recurrence along the tract of the initial surgical route, and CT on the day after the second surgery demonstrated no remarkable calcification. However, the possibility of missing minute calcification is quite high. A few areas of calcification had to exist in the surgical tract for ectopic recurrence. It is therefore possible that the Ommaya reservoir cannula, which was placed within the same surgical route, might have played a role in this ectopic recurrence because of the very short time to seeding and the findings on CT and MR images.

The careful handling of tumor fragments during surgical procedures and irrigation of the surgical site are important operative steps to prevent this rare complication.

References

1 Burger PC, Scheithauer BW, Vogel FS: Surgical Pathology of the Nervous System and Its Coverings, ed 3. New York, Churchill Livingstone, 1991, pp 700–709.
2 Petito CK, DeGirolami U, Earle KM: Craniopharyngiomas. A clinical and pathological review. Cancer 1976;37:1944–1952.
3 Russell DS, Rubinstein LJ: Pathology of Tumors of the Nervous System, ed 5. Baltimore, Williams and Wilkins, 1989, pp 695–702.
4 Barloon TJ, Yuh WT, Sato Y, Sickels WJ: Frontal lobe implantation of craniopharyngioma by repeated needle aspiration. AJNR Am J Neuroradiol 1988;9:406–407.
5 Freitag SK, Miller NR, Brem H: Recurrent ectopic craniopharyngioma. Br J Neurosurg 2001;15:511–513.
6 Gupta K, Kuhn MJ, Shevlin DW, Wacaser LE: Metastatic craniopharyngioma. AJNR Am J Neuroradiol 1999;20:1059–1060.
7 Israel ZH, Pomerantz S: Intracranial craniopharyngioma seeding following radical resection. Pediatr Neurosurg 1995;22:210–213.
8 Ito M, Jamshidi J, Yamanaka K: Does craniopharyngioma metastasize? Case report and review of the literature. Neurosurgery 2001;48: 933–935.
9 Lee DK, Jung H, Kim DG, Paek SH, Gwak H, Choe G: Postoperative spinal seeding of craniopharyngioma. Case report. J Neurosurg 2001;94:617–620.
10 Lee JH, Kim CY, Kim DG, Jung H: Postoperative ectopic seeding of craniopharyngioma. Case illustration. J Neurosurg 1999;90:796.
11 Liu JM, Garonzik IM, Eberhart CG, Sampath P, Brem H: Ectopic recurrence of craniopharyngioma after an interhemispheric transcallosal approach. Case report. Neurosurgery 2002; 50:639–645.
12 Malik JM, Cosgrove GR, VandenBerg SR: Remote recurrence of craniopharyngioma in the epidural space. Case report. J Neurosurg 1992; 77:804–807.
13 Nomura H, Kurimoto M, Nagai S, Hayashi N, Hirashima Y, Tsukamoto E, Endo S: Multiple intracranial seeding of craniopharyngioma after repeated surgery. Case report. Neurol Med Chir (Tokyo) 2002;42:268–271.
14 Ragoowansi AT, Piepgras DG: Postoperative ectopic craniopharyngioma. Case report. J Neurosurg 1991;74:653–655.
15 Tomita S, Mendoza ND, Symon L: Recurrent craniopharyngioma in the posterior fossa. Br J Neurosurg 1992;6:587–590.
16 Bleyer WA, Pizzo PA, Spence AM, Platt WD, Benjamin DR, Kolins J, Poplack DG: The Ommaya reservoir. Newly recognized complications and recommendations for insertion and use. Cancer 1978;41:2431–2437.

日本小児科学会雑誌　108巻7号　1001～1005（2004年）

小児医療

地方大学附属病院における小児救急医療体制の問題点

大分大学医学部脳神経機能統御講座小児科学[1]，大分こども病院小児科[2]，
大分市医師会立アルメイダ病院小児科[3]
末延　聡一[1]　前田　知己[1]　是松　聖悟[1]　今井　一秀[1]
秋吉　健介[1]　高橋　瑞穂[1]　曽根　律子[1]　石原　高信[1][2]
福島　直喜[1][3]　古城　昌展[1]　泉　達郎[1]

要　旨

大学附属病院における最近5年間の時間外診療における，小児救急受診状況を調査した．時間外外来受診者数は小児科が常に最多で，内科3科合計，外科3科合計よりも多数であった．しかし救急講座は心臓血管外科医が中心で，小児科出身のスタッフはいない．同時に時間外を含む一次診療を担当する総合診療部も同様に内科医が中心で小児科医はいない．これらの診療科は最近新設されたものであるが，大学附属病院における小児科学講座教官定員の削減とともに，小児科医対内科・外科医の比率は減少しており，小児科医志望の学生の減少，小児科医不足の一因となっていると考えた．大学附属病院の救急外来や総合診療部はそれぞれ外科医と内科医が中心で，小児科医はいない事は患者数の比率からも不適当であり，これらの科にも小児科出身の専任医が必要である．そうすることにより大学附属病院救急外来の充実につながり，ひいては多くの若い小児科医たちを増やすことが出来ると考える．

キーワード：小児時間外救急，小児科医師不足，小児医療の充実

はじめに

少子高齢化，不採算ゆえの病院小児科の閉鎖，小児時間外救急体制の不備等が指摘されて久しい[1][2]．安心してこどもを生み，育てる環境すなわち小児の救急医療の充実こそが21世紀の基礎であると考え，この問題点を明確にするため大分医科大学（2003年10月1日より大分大学）附属病院における小児科の時間外救急対応状況を，他科と比較し分析した．

小児救急医療における時間外診療体制の最大の問題点は小児科医不足であるという指摘は随所でなされている．まず，小児科医を希望する学生が増加するためには教育・研修を担う大学附属病院小児科が，活動的で，臨床・研究ともに将来性があり，継続的に貢献するに値しうる魅力的な科であるかを検討するために，我々小児科医や大学附属病院が担っている現状を検討した．

対象と方法

1998年4月から2003年3月までの間に，平日8：30から17：00以外の時間に大分医科大学附属病院の救急部を受診（以下，時間外救急）した外来患者，計26284名を対象とした．これらの患者の内訳を診療科別に分け，時間外救急患者総数，救急車を利用した時間外救急患者数，時間外救急患者の入院数を検討した．

結　果

当院は大分市と大分郡の中間に位置している．診療科は21あり，内訳は，小児科，内科（1），内科（2），内科（3），外科（1），外科（2），心臓血管外科，産婦人科，眼科，耳鼻咽喉科，精神科神経科，脳神経外科，整形外科，皮膚科，泌尿器科，放射線科，麻酔科，臨床薬理，歯科口腔外科，総合診療部および救急医学講座である．

2002年4月から2003年3月の1年間における21診療科の平均在院日数は22.0日，病床稼働率は85.8%だった．小児科単科では平均在院日数は20.1日，病床稼働率は99.9%だった．

1．2002年度時間外救急患者数（図1）

2002年度診療科別時間外救急患者数を示す．小児科の時間外救急患者数は1,184名で，内科3科の総計962名，心臓血管外科を含む外科3科の総計809名よりも多数であった．全21診療科中小児科受診が最多，続いて眼科，産婦人科，耳鼻咽喉科であった．過去4年間

（平成16年1月19日受付）（平成16年5月13日受理）
別刷請求先：（〒879-5593）大分郡挾間町医大ヶ丘1—1
大分大学医学部脳神経機能統御講座小児科学
末延　聡一

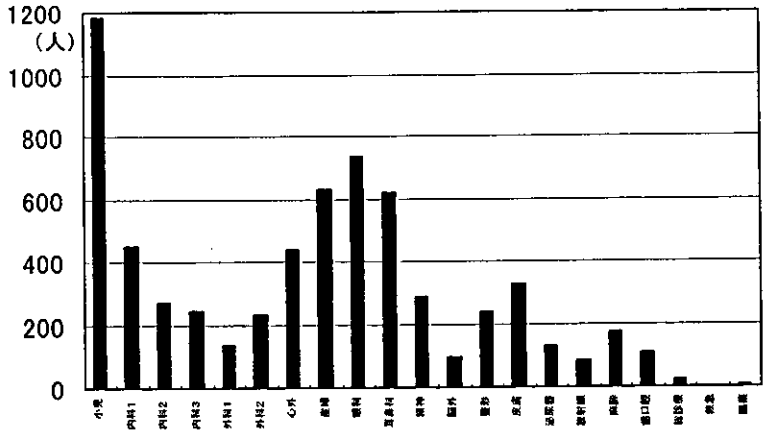

図1　2002年度時間外救急患者数

2002年度診療科別時間外救急患者数を示す．小児科の時間外救急患者数は1,184名で，内科3科の総計962名，心臓血管外科を含む外科3科の総計809名よりも多数であった．全21診療科中小児科受診が最多，続いて眼科，産婦人科，耳鼻咽喉科であった．過去4年間いずれもこの4科が1～4位だったので，以後の検討はこの4診療科と内科3科，外科3科を加えた6部門にて行った．

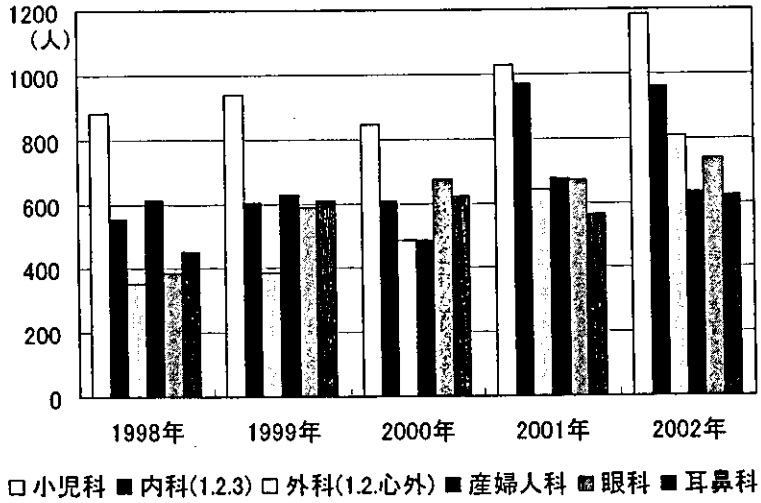

図2　小児科，内科，外科，産婦人科，眼科，耳鼻咽喉科の時間外救急患者数の推移(1998～2002年度)

6部門の過去5年間の時間外救急患者数を示す．2位以下は年度別の変動があったが，小児科の患者数は4年間常に最多で，年平均976名だった．

いずれもこの4科が1～4位だったので，以後の検討はこの4診療科と内科3科，外科3科を加えた6部門にて行った．

2．小児科，内科，外科，産婦人科，眼科，耳鼻咽喉科の時間外救急患者数の推移（図2）

6部門の過去5年間の時間外救急患者数を示す．2位以下は年度別の変動があったが，小児科の患者数は4年間常に最多で，年平均976名だった．

3．小児科，内科，外科，産婦人科，眼科，耳鼻咽喉科の救急車を利用した時間外救急患者数の推移（図3）

6部門の過去4年間の救急車を利用した受診者数の推移を示す．小児科は3位で，年平均63件だった．

4．小児科，内科，外科，産婦人科，耳鼻科，眼科の時間外救急患者の入院数の推移（図4）

6部門の過去5年間の時間外救急からの入院数の推移を示す．小児科入院数は年間104～184名（年平均128名）で，内科，外科，産婦人科と同等であった．なお，時間外救急患者の入院数には，新生児の緊急入院および救急部を経由しない，病棟への直接入院は含まない．

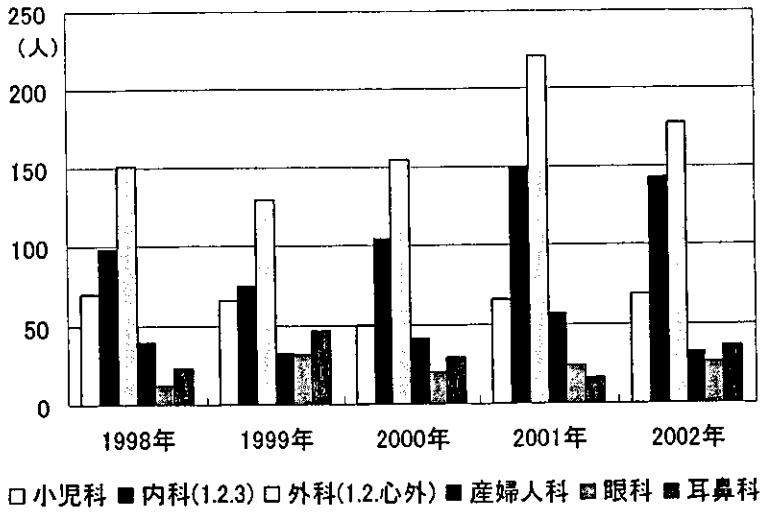

図3　小児科，内科，外科，産婦人科，眼科，耳鼻咽喉科の救急車を利用した時間外救急患者数の推移（1998～2002年度）
6部門の過去4年間の救急車を利用した受診者数の推移を示す．小児科3位で，年平均63件だった．

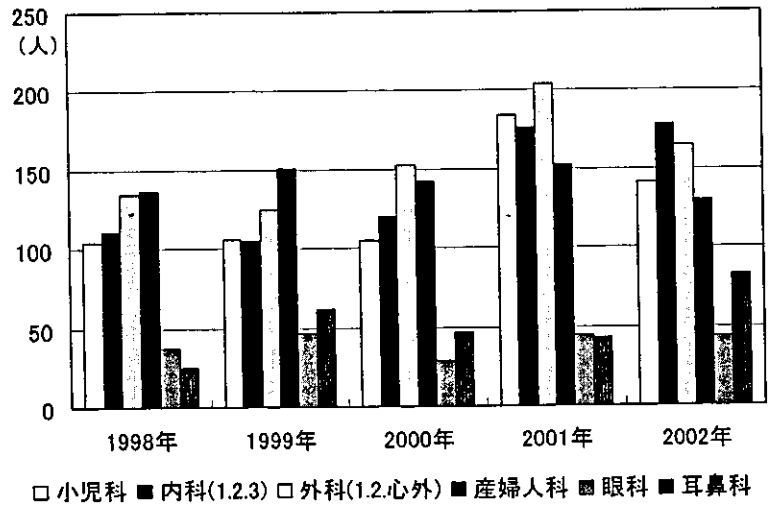

図4　小児科，内科，外科，産婦人科，耳鼻科，眼科の時間外救急患者の入院数の推移（1998～2002年度）
6部門の過去5年間の時間外救急からの入院数の推移を示す．小児科入院数は年間104～184名（年平均128名）で，内科，外科，産婦人科と同等であった．なお，時間外救急患者の入院数には，新生児の緊急入院および救急部を経由しない，病棟への直接入院は含まない．

考　察

小児救急医療には痙攣重積症や溺水，急性脳炎・脳症など真の救急集中治療を要するものと，女性，母親の社会進出，核家族化などの社会情勢の変化に伴う小児時間外診療がある．大部分が後者であるがゆえに小児科医による対応が必要であり，慢性的な少子高齢過疎化を呈す市町村においても，安心してこどもを産み，育てられる環境の構築には小児医療の充実は必須である．小児科医を志望する学生を教育し，若い小児科医を研修育成する立場にある当院における小児救急医療体制に関する問題点を示す．

小児救急医療の重要性が広く指摘されている中で，当大学のような，いわゆる新設医科大学では，限られた教官数のなかで，新しい講座や診療科の増設がなされているが，最近新設された救急医学講座と総合診療部の教官は，小児科をはじめとする各科よりの定員削減・供出から成り，それぞれ心臓血管外科医と内科医

を中心としている．小児科出身の医員・教官は不在であり，小児科教官の減少となっている．図1に示したように，救急受診患者の中で小児科受診患者数が最多であるにもかかわらず，当院においては救急医学講座に小児科医の専任教官はいない．総合診療部も同様である．大学附属病院を救急医，総合医，家庭医の教育育成を目的とするならば，小児科医もその一端を担うべきであり，内科医・外科医も将来，救急医や総合医を目指すのであれば，尚更小児救急研修の指導は小児科医が責を負うべきであろう．

当院小児科病棟では難治性てんかん等の神経疾患や血液腫瘍性疾患，新生児集中治療室（NICU）への入院などが主体を占める．常時，多数の人工呼吸器が稼動している重症で多忙な病棟やそれらの当直業務のなかで，更に救急患者の対応をする必要があるという二重構造は大学附属病院における小児救急の大きな問題点である．時間外受診した小児を総合診療医すなわち家庭医，または小児科専門医として適確に診療し，教育研修するためには小児科医の教官や医員数の確保が必要であるが，その絶対数は不足している．これを裏付ける資料として，全国的に，附属病院内にある救急医学，救急科，およびそれに類する診療単位の教官の出身診療科を主な研究領域から類推した．小児科出身者は全74名の教授の中でわずか3名（4%），助教授に至っては63名中1名だった[3]．

次に，保険診療費の廉価である．2002年度の診療報酬改正では，地域の小児科医の参加する小児夜間・休日診療体制の評価や，小児入院医療管理料の加算項目追加など，小児科に有利な改正も行われたが，薬剤の投与量が少なく，急性疾患が主体の小児救急医療に限らず，小児医療全体の問題としていまだ薬価や小児科医としての手技料や技術料は算定に考慮されてはいるが，過少である．小児科専門医としての優遇措置も考慮されるべきである．

さらに，内科医と小児科医の認識の相違が挙げられる．内科医がどこまで小児疾患に関わることができるかについては個々の医師の資質にもよる．現在，救急告示病院において小児の救急患者を受け入れている病院は53.7%のみという報告があり[6]，救急告示病院ですら，小児救急診療の不備は明らかである．米国のように，救急部には小児科診療の研修を受けた救急医や総合診療医が常駐し，小児患者の診察を拒否すると違法行為になるようなシステムもわが国には無く[5]，必然的に夜間診療の小児科医への負担は大きくなる．当院では，本来，救急部や総合診療部の専任医師が一次診療をすべき時間外小児患者を，小児科当直医がオンコール体制の下で最初に診察している．この不備を解決するには最終的には小児科医の数的充足が不可欠であり[6,7]，教官数の増多が望まれる．また，そのためには小児を診療する行為そのものに対する公費負担制度つまり小児科専門医に対する診療報酬の底上げは必須である．これらは本邦における大学附属病院全体に共通する課題であろう．

さて，当大分県では主たる診療科目を小児科とする「小児科医」は132名いるが，その大部分は都市部，大分（63名），別府（28名），中津下毛（12名）の各2次医療圏（保健医療圏）に偏在している．竹田直入（0名），東国東（1名）の保健医療圏をはじめとする小児科過疎地域は少子，高齢，過疎化の急速な促進がみられる．これらの地域における小児医療への貢献の重要性は地域住民だけでなく，行政，当小児科医局全体の一致した認識であり，少子，高齢，過疎化の急速な促進ゆえに小児科過疎となる地域への貢献もまた地方大学病院の使命の一部である．

結　語

1. 大分大学医学部附属病院における救急診療の状況について調査した．時間外救急患者総数は小児科が最多で，これは内科3科の総外来数より多かった．

2. 小児救急医療体制に関する問題点としては救急医学講座，総合診療部における小児科の教官，小児科医師の不足，保険診療費の廉価などが挙げられる．

3. 我々小児科医としては，今後多忙な小児救急体制を改善すべく，社会に働きかける必要がある．また，我々小児科医も意識改革の必要がある．

4. 諸外国のような大学附属小児病院とまではいかなくとも，本邦におけるこどもの医療環境，家庭・社会環境の改善には，小児科医療スタッフ，教官の増員が必要である．

本稿の要旨は，第105回日本小児科学会学術集会（2002年4月，名古屋市）において報告した．

文　献

1) 市川光太郎．小児救急の原点．小児科診療 2001；11：1647—1657.
2) 田中哲郎．小児救急における理想像．小児科診療 2001；11：1652—1657.
3) 葛西文明．医育機関名簿 2001-2002．東京．羊土社，2001.
4) 田中哲郎．21世紀の小児救急医療．日児誌 2002；106：721—729.
5) 大矢幸弘，広瀬輝夫，飯倉洋治，他．プライマリーケア，救急医療，専門医の3役を欧米の半分以下でこなす日本の小児科医．日児誌 2002；106：2—7.
6) 田中哲郎，市川光太郎，山田至康．小児救急医療における小児科医不足—医学部学生の小児科に対する考え方—．日本医事新報 2001；4017：37—43.

7) 柳澤正義, 前川喜平, 天野 曄. 小児救急医療体制に関する要望. 2001；小児救急医療に関する要望書. 厚生労働省雇用均等・児童家庭局長宛, 厚生労働省医政局宛.

The Pediatric Emergency Clinic ; Its Evaluations and the Proposals for the Improvement at Oita Medical University Hospital, Department of Pediatrics

Souichi Suenobu[1], Tomoki Maeda[1], Seigo Korematsu[1], Kazuhide Imai[1], Kensuke Akiyoshi[1], Mizuho Takahashi[1], Ritsuko Sone[1], Takanobu Ishihara[1)2)], Naoki Fukushima[1)3)], Masanobu Kojo[1] and Tatsuro Izumi[1]

[1]Department of Brain and Nerve Science, Department of Pediatrics, Oita University Faculty of Medicine

[2]Department of Pediatrics, Oita Children's Hospital

[3]Department of Pediatrics, Almeida Hospital

Here we evaluated the real state of pediatric emergency clinic at Oita Medical University Hospital for these five years. In our University hospital, we pediatricians has been called most frequent and busy in the extra-time emergency clinic than the other doctors of the physician, surgeon, cardiologist, neurosurgeon et al.

Nevertheless, in the Departments of Emergency Medicine and General Medicine, which were recently established for the emergency clinic and primary care, these departments' staffs were occupied by the surgeons and physicians without any staff of pediatrician. For both of the improvement of pediatric emergency clinic and the increasement of young pediatricians, it might be essential to install and increase the pediatric staffs in Departments of Emergency Medicine, General Medicine, and also Pediatrics including NICU of the University Hospital.